Interpretation of the UV−vis Spectra of the meso(Ferrocenyl)-Containing Porphyrins using a TDDFT Approach: Is Gouterman's Classic Four-Orbital Model Still in Play?

ARTICLE *in* THE JOURNAL OF PHYSICAL CHEMISTRY A · OCTOBER 2010

Impact Factor: 2.69 · DOI: 10.1021/jp1083828 · Source: PubMed

2 AUTHORS:

Victor N Nemykin
University of Minnesota Duluth
202 PUBLICATIONS **2,643** CITATIONS
SEE PROFILE

Ryan G Hadt
Argonne National Laboratory
33 PUBLICATIONS **956** CITATIONS
SEE PROFILE

Interpretation of the UV−vis Spectra of the *meso*(Ferrocenyl)-Containing Porphyrins using a TDDFT Approach: Is Gouterman's Classic Four-Orbital Model Still in Play?

Victor N. Nemykin* and Ryan G. Hadt

Department of Chemistry and Biochemistry, University of Minnesota−Duluth, Duluth, Minnesota 55812, United States

Received: September 2, 2010; Revised Manuscript Received: October 7, 2010

The vertical excitation energies of H_2TPP [TPP = 5,10,15,20-tetraphenylporphyrin(2-)], H_2FcPh$_3$P [FcPh$_3$P = 5-ferrocenyl-10,15,20-triphenylporphyrin(2-)], *cis*-$H_2Fc_2Ph_2P$ [*cis*-Fc_2Ph_2P = 5,10-bisferrocenyl-15,20-diphenylporphyrin (2-)], *trans*-$H_2Fc_2Ph_2P$ [*trans*-Fc_2Ph_2P = 5,15-bisferrocenyl-10,20-diphenylporphyrin-(2-)], H_2Fc_3PhP [H_2Fc_3PhP = 5,10,15-trisferrocenyl-20-phenylporphyrin(2-)], and H_2TFcP [TFcP = 5,10,15,20-tetraferrocenylporphyrin(2-)] were investigated using a time-dependent density functional theory (DFT) approach and compared to their experimental UV−vis spectra in the 10 000−30 000 cm^{-1} region. It was shown that the lowest energy transitions in *meso*(ferrocenyl)-containing porphyrins have predominantly ferrocene-to-porphyrin charge transfer character, while the porphyrin-centered $\pi-\pi^*$ transitions predicted by the Gouterman's classic four-orbital model still have the largest intensities in the UV−vis region. The number of predominantly ferrocene-to-porphyrin charge transfer transitions increases with the number of ferrocene substituents and becomes dominant in H_2TFcP.

Introduction

Developed in the 1960s by Gouterman, the four-orbital model[1] is probably the most widely used theory for the interpretation of the UV−vis spectra of porphyrins, phthalocyanines, and related compounds.[2] This model aids in understanding the key features in the 10 000−30 000 cm^{-1} region of the UV−vis spectra of porphyrinoids by considering excited states originating from transitions between the porphyrin core-centered HOMO and HOMO-1 π orbitals and LUMO and LUMO+1 π^* orbitals (Figure 1). In the case of transition-metal porphyrins with an effective 4-fold (i.e., D_{4h}) symmetry, the LUMO and LUMO+1 MOs are degenerate by symmetry (these are labeled as e_{gx} and e_{gy} in Figure 1), whereas the HOMO and HOMO-1 are nearly degenerate. Excited states originating from $a_{1u} \rightarrow e_{gy}$ and $a_{2u} \rightarrow e_{gx}$ transitions have x-polarization, while those between $a_{1u} \rightarrow e_{gx}$ and $a_{2u} \rightarrow e_{gy}$ orbitals are *y*-polarized. *x*- and *y*-polarized excited states are further mixed and split in energy by configuration interaction into two pairs of degenerate ^1E_u low-energy, low intensity (Q_x and Q_y) and high-energy, high intensity (B_x and B_y also known as Soret band) transitions.[1] Lowering the effective symmetry in metal-free porphyrins from D_{4h} to D_{2h} results in nondegeneracy of the LUMO and LUMO+1 MOs and further splitting of Q_x and Q_y as well as B_x and B_y transitions (Figure 1). In order to avoid confusion, when the target low-symmetry porphyrins are discussed below, the generalized notation proposed by Gouterman[1] will be used (i.e., b_1, b_2, c_1, and c_2 for a_{1u}, a_{2u}, e_{gx}, and e_{gy} (D_{4h} symmetry) and a_u, b_{1u}, b_{3g}, and b_{2g} (D_{2h} symmetry) MOs) (Figure 1).

Ferrocenyl-containing porphyrins,[3−5] corroles,[6] tetraazaporphyrins,[7] phthalocyanines,[8] and their nonaromatic analogues[9] with direct ferrocene-macrocycle bond(s) represent an exciting class of macrocyclic compounds.[10] It was shown that the redox-active ferrocene group(s) in these complexes control their redox behavior, optical and fluorescence properties, as well as provide a potential access to photoinduced electron transfer processes, unpaired electron density migration, and long-range metal−metal coupling.[3,10] These stable, rigid, and nearly planar macrocyclic nanomeric size redox- and optically driven switchable modules could also be used in molecular-based electronic devices such as molecular multibit storage elements, molecular electrogenic sensors, and molecular arrays that mimic photosynthetic active sites.[11] Although UV−vis spectra of the *meso*(ferrocenyl)-containing porphyrins[3] are similar to other *meso*(aryl)-containing porphyrins, several striking differences should be pointed out. As the number of ferrocene substituents in *meso*(ferrocenyl)-containing porphyrins increases, both the Q- and B-bands undergo a low-energy shift, the Q bands become more intense and broad, and an additional broad shoulder between 450 and 500 nm appears in the UV−vis spectra. While the low-energy shift of Q- and B-bands could be explained as a function of nonplanarity of the porphyrin core, the appearance of a broad shoulder between the B- and Q-bands as well as broadening of the Q-bands cannot be easily explained. One of the possible reasons for such spectroscopic behavior of the *meso*(ferrocenyl)-containing porphyrins could be the presence of ferrocene-centered MOs located between the classic Gouterman-type porphyrin-centered π and π^* MOs. This hypothesis was recently confirmed by electrochemical, spectroelectrochemical, XPS and Mössbauer methods.[3m,o] Such a situation could potentially result in numerous ferrocene-to-porphyrin charge-transfer transitions with energies close to the Q-bands thus complicating UV−vis spectra of the *meso*(ferrocenyl)-containing porphyrins. In order to clarify band assignments in *meso*-(ferrocenyl)-containing porphyrins, we used a time-dependent DFT (TDDFT) approach and calculated vertical excitation energies of H_2TPP [TPP = 5,10,15,20-tetraphenylporphyrin(2-)], H_2FcPh$_3$P [FcPh$_3$P = 5-ferrocenyl-10,15,20-triphenylporphyrin(2-)], *cis*-$H_2Fc_2Ph_2P$ [*cis*-Fc_2Ph_2P = 5,10-bisferrocenyl-15,20-diphenylporphyrin (2-)], *trans*-$H_2Fc_2Ph_2P$ [*trans*-Fc_2Ph_2P = 5,15-bisferrocenyl-10,20-diphenylporphyrin(2-)], H_2Fc_3PhP [H_2Fc_3PhP = 5,10, 15-trisferrocenyl-20-phenylporphyrin(2-)], and H_2TFcP [TFcP = 5,10,15,20-tetraferrocenylporphyrin(2-)].

* Corresponding author. E-mail: vnemykin@d.umn.edu.

10.1021/jp1083828

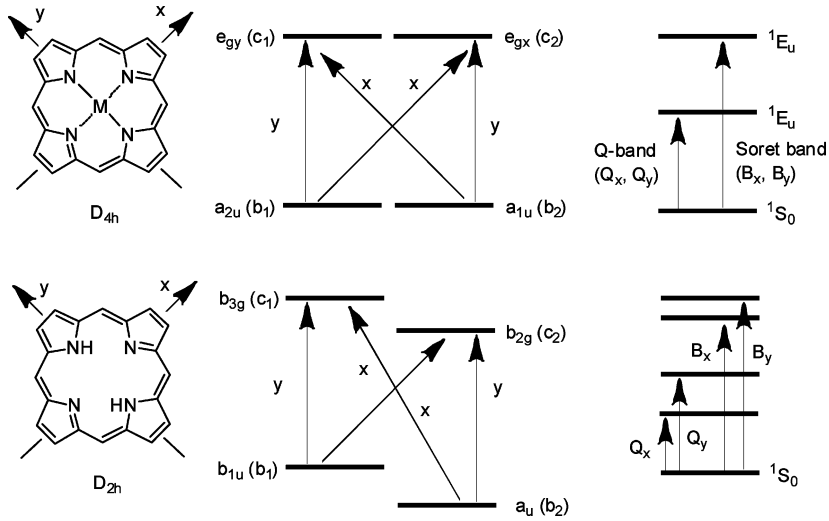

Figure 1. Simplified Gouterman's four-orbital model for transition-metal D_{4h} symmetry porphyrins (top) and D_{2h} symmetry metal-free porphyrins (bottom).

Experimental Section

Synthesis and Instrumentation. Target H_2FcPh_3P, *cis*-$H_2Fc_2Ph_2P$, *trans*-$H_2Fc_2Ph_2P$, H_2Fc_3PhP, H_2TFcP were prepared earlier in our laboratory using cross-condensation reaction between pyrrole, benzaldehyde and ferrocenecarbaldehyde.[12] UV−vis−NIR data were obtained on Jacso V-670 or Cary 17 spectrometers in dichloromethane as solvent. MCD data were recorded using an OLIS DCM 17 CD spectropolarimeter using a permanent 1.4 T DeSa magnet. The spectra were recorded twice for each sample, once with a parallel field and again with an antiparallel field, and their intensities were expressed by molar ellipticity per T = [Θ]M/deg dm^3 mol^{-1} cm^{-1} T^{-1}.

Computational Aspects. All DFT calculations were conducted using the Gaussian 03 software package running under either a Windows or UNIX OS.[13] The molecular geometries were obtained via optimization with Becke's exchange functional[14] and the Perdew nonlocal correlation functional (BPW91)[15] coupled with Wachter's full-electron basis set for the iron[16] atom and the 6-31G(d) basis set[17] for all other atoms. For all optimized structures, frequency calculations were carried out to ensure that optimized geometries represented local minima. When necessary, the percent contributions of atomic orbitals to molecular orbitals were calculated using the VMOdes program.[18] TDDFT calculations were conducted at the same level of theory as geometry optimizations and single point calculations. The first 40 (H_2TPP), 50 (H_2FcPh_3P), 60 (*cis*-$H_2Fc_2Ph_2P$), 60 (*trans*-$H_2Fc_2Ph_2P$), 80 (H_2Fc_3PhP), and 100 (H_2TFcP) excited states were calculated in order to ensure that both Q- and B-band regions are covered.

Results and Discussion

The vertical excitation energies in target metal-free *meso*-(ferrocenyl)-containing porphyrins (Figure 2) were calculated using a TDDFT approach coupled with a GGA exchange-correlation functional and relatively large basis set. Such combination of exchange-correlation functional and basis set has proven to provide reliable agreement between predicted and experimentally observed vertical excitation energies and other spectroscopic properties in porphyrinoids and ferrocene-containing compounds, although in some cases systematic errors for the predicted energies have been observed.[19,20] The MO diagrams for the target metal-free *meso*(ferrocenyl)-containing porphyrins and the reference H_2TPP are presented in Figure 3

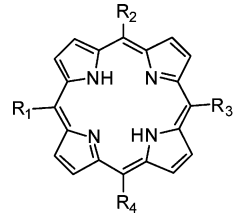

H_2TPP:	R_1 - R_4 = Ph
H_2FcPh_3P:	R_1 = Fc; R_2 - R_4 = Ph
cis-$H_2Fc_2Ph_2P$:	R_1 = R_2 = Fc; R_3 = R_4 = Ph
trans-$H_2Fc_2Ph_2P$:	R_1 = R_3 = Fc; R_2 = R_4 = Ph
H_2Fc_3PhP:	R_1 - R_3 = Fc; R_4 = Ph
H_2TFcP:	R_1 - R_4 = Fc

Figure 2. Target metal-free *meso*(ferrocenyl)-containing porphyrins and reference compound.

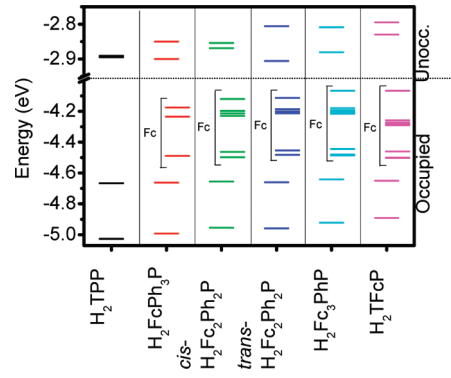

Figure 3. Partial molecular orbital diagram for *meso*(ferrocenyl)-containing porphyrins and reference H_2TPP.

with an analysis of the orbital composition in the Supporting Information, Figure 1. In addition, the frontier orbitals of the target porphyrins are pictured in the Supporting Information, Figure 2. In agreement with Gouterman's classic four-orbital model for porphyrins,[1] the HOMO and HOMO-1 in H_2TPP are porphyrin-based π-orbitals, which correspond to b_{1u} and a_u MOs in the D_{2h} point group notation. Introduction of a single ferrocene substituent onto the porphyrin core in H_2FcPh_3P results in the HOMO to HOMO-2 becoming predominantly iron-centered (d_{xy}, $d_{x^2-y^2}$, and d_{z^2}) MOs while the classic porphyrin core-centered occupied π-orbitals are located at lower energies. Similarly, six predominantly ferrocene centered MOs were observed as HOMO to HOMO-5 in *cis*-$H_2Fc_2Ph_2P$ and *trans*-$H_2Fc_2Ph_2P$ (three MOs per ferrocene substituent), nine predominantly ferrocene centered MOs were observed as HOMO to HOMO-8 in H_2Fc_3PhP, and twelve predominantly ferrocene centered MOs were observed as HOMO to HOMO-11 in H_2TFcP (Figures 3 and SI Figure 1). In general, the energy of the predominantly

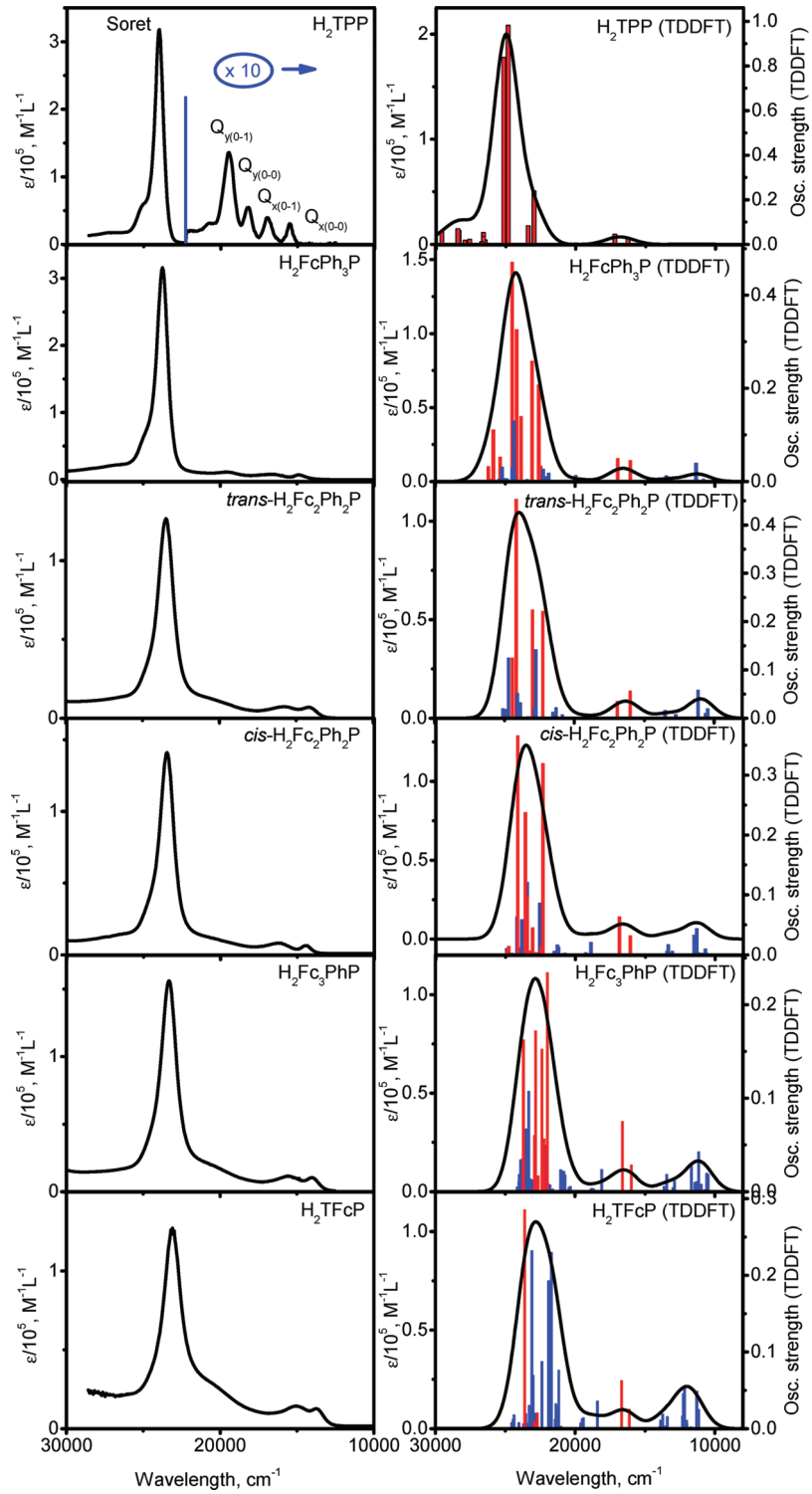

Figure 4. Experimental (left) and TDDFT predicted (right) UV−vis spectra of the *meso*(ferrocenyl)-containing porphyrins and reference H_2TPP. Solid black lines represent experimental (left) or simulated (right; line broadening = 1000 cm^{-1}) data, vertical red bars represent predominantly $\pi-\pi^*$ transitions, and vertical blue bars represent predominantly MLCT transitions.

ferrocene-based HOMO increases with the number of ferrocene substituents. Although the HOMO in all *meso*(ferrocenyl)-containing porphyrins is predominantly ferrocene-based, the porphyrin core π-orbital contribution gradually increases with the number of ferrocene substituents. Indeed, it is ~10% in H_2FcPh_3P, ~14−16% in $H_2Fc_2Ph_2P$, ~20% in H_2Fc_3PhP, and ~30% in H_2TFcP. In agreement with previous computational data,[3m,o] the LUMO and LUMO+1 in *meso*-(ferrocenyl)-containing porphyrins are close in energy and predominantly porphyrin based Gouterman's type π^*-orbitals. In all cases, these MOs are energetically well separated from higher energy unoccuppied orbitals (LUMO+2 and above).

The TDDFT predicted vertical excitation energies for metal-free *meso*(ferrocenyl)-containing porphyrins and the reference H_2TPP are shown in Figure 4 along with individual experimental UV−vis spectra. In agreement with its electronic structure, all intense transitions in the reference H_2TPP are $\pi-\pi^*$ in nature with typical TDDFT errors in a very reasonable range of ~0.1

eV. Expectedly, the most intense $\pi-\pi^*$ transitions predicted by TDDFT in the Q- and Soret band area are in agreement with Gouterman's four-orbital model and originate from HOMO and HOMO-1 to LUMO and LUMO+1 excitations (SI Table 1). The presence of three predominantly ferrocene-centered HOMO to HOMO-2 MOs in H_2FcPh_3P results in six transitions with predominantly MLCT character (bands 1−6, SI Table 2) located at lower energies as compared to the TDDFT predicted $\pi-\pi^*$ Q-bands (transitions 7 and 8, SI Table 2). In addition, several intense transitions with predominant MLCT character were also predicted by TDDFT between the Q- and the Soret bands although Gouterman's classic $\pi-\pi^*$ transitions retain the largest intensities in the regions of both the Q- and Soret bands (Figure 4). Similarly, in the case of *cis*-$H_2Fc_2Ph_2P$ and *trans*-$H_2Fc_2Ph_2P$ complexes, transitions from six predominantly ferrocene-centered HOMO to HOMO-5 to porphyrin-core π^* LUMO and LUMO+1 result in twelve low-energy bands with predominant MLCT character prior to the pure $\pi-\pi^*$ Q-bands (transitions 13 and 14). In the Soret band region, four $\pi-\pi^*$ transitions provide the largest contribution to the overall intensity, while numerous predominantly MLCT bands are responsible for the prominent shoulder observed experimentally between 470 and 500 nm. Again, the intensities of the $\pi-\pi^*$ transitions are larger as compared to MLCT bands in the Q- and Soret band regions. The presence of three ferrocene substituents in H_2Fc_3PhP results in the TDDFT predicted 18 low-energy MLCT transitions from mainly ferrocene-centered HOMO to HOMO-8 to the porphyrin-centered π^* LUMO and LUMO+1. These are followed by two classic $\pi-\pi^*$ Q-bands (transitions 19 and 20, SI Table 5). The last two transitions along with the four most intense $\pi-\pi^*$ transitions located in the Soret band region prevail over the UV−vis spectrum of H_2Fc_3PhP. Finally, transitions from twelve mainly ferrocene-centered HOMO to HOMO-11 to the porphyrin-centered LUMO and LUMO+1 MOs in H_2TFcP result in 24 predominantly MLCT bands in the UV−vis spectrum located at lower energies as compared to the classic $\pi-\pi^*$ Q-bands (bands 25 and 26, SI Table 6). More importantly, the Soret band region of the H_2TFcP spectrum is also dominated by MLCT bands with only one intense predominantly $\pi-\pi^*$ transition. It should be noted that although within typical TDDFT errors, the vertical excitation energies of the low-energy MLCT transitions are underestimated by the TDDFT method predominantly because of the inherent difficulties associated with DFT and TDDFT methods such as the self-interaction error[21] and the inability to adequately model charge-transfer over larger distances.[22]

Conclusions

Overall, TDDFT calculations have clearly explained the differences between UV−vis spectra of the metal-free tetra(aryl)porphyrins and the new *meso*(ferrocenyl)-containing porphyrins. Indeed, the appearance of a broad shoulder between the Soret- and Q- bands as well as broadening in the Q-band regions can now be assigned to the ferrocene-to-porphyrin charge transfer bands. The number of such bands increases with the number of ferrocene substituents and they become dominant in the UV−vis spectrum of H_2TFcP.

Acknowledgment. Generous support from NSF (CHE-0809203) and Minnesota Supercomputing Institute is greatly appreciated. We also would like to thank Dr. Rodion Belosludov and Dr. Douglas Fox for help with several TDDFT calculations.

Supporting Information Available: Computational details, molecular orbital compositions, and tabulated TDDFT data for target compounds. This material is available free of charge via the Internet at http://pubs.acs.org.

References and Notes

(1) Gouterman, M. *J. Mol. Spectrosc.* **1961**, *6*, 138–163.

(2) Cheek, J.; Dawson, J. H. In *Porphyrin Handbook*; Kadish, K. M., Smith, K. M., Guillard, R., Eds.; Academic Press: New York, 2000; Vol. 7, pp 339−369.

(3) (a) Bucher, C.; Devillers, C. H.; Moutet, J.-C.; Royal, G.; Saint-Aman, E. *Coord. Chem. Rev.* **2009**, *253*, 21–36. (b) Loim, N. M.; Abramova, N. V.; Sokolov, V. I. *Mendeleev Commun.* **1996**, 46–47. (c) Burrell, A. K.; Campbell, W. M.; Jameson, G. B.; Officer, D. L.; Boyd, P. D. W.; Zhao, Z.; Cocks, P. A.; Gordon, K. C. *Chem. Commun.* **1999**, 637–638. (d) Narayanan, S. J.; Venkatraman, S.; Dey, S. R.; Sridevi, B.; Anand, V. R. G.; Chandrashekar, T. K. *Synlett* **2000**, 1834–1836. (e) Rhee, S. W.; Na, Y. H.; Do, Y.; Kim, J. *Inorg. Chim. Acta* **2000**, *309*, 49–56. (f) Shoji, O.; Okada, S.; Satake, A.; Kobuke, Y. *J. Am. Chem. Soc.* **2005**, *127*, 2201–2210. (g) Shoji, O.; Tanaka, H.; Kawai, T.; Kobuke, Y. *J. Am. Chem. Soc.* **2005**, *127*, 8598–8599. (h) Auger, A.; Swarts, J. C. *Organometallics* **2007**, *26*, 102–109. (i) Kubo, M.; Mori, Y.; Otani, M.; Murakami, M.; Ishibashi, Y.; Yasuda, M.; Hosomizu, K.; Miyasaka, H.; Imahori, H.; Nakashima, S. *J. Phys.Chem. A* **2007**, *111*, 5136–5143. (j) Nemykin, V. N.; Barrett, C. D.; Hadt, R. G.; Subbotin, R. I.; Maximov, A. Y.; Polshin, E. V.; Koposov, A. Y. *Dalton Trans.* **2007**, 3378–3389. (k) Rochford, J.; Rooney, A. D.; Pryce, M. T. *Inorg. Chem.* **2007**, *46*, 7247–7249. (l) Nemykin, V. N.; Galloni, P.; Floris, B.; Barrett, C. D.; Hadt, R. G.; Subbotin, R. I.; Marrani, A. G.; Zanoni, R.; Loim, N. M. *Dalton Trans.* **2008**, 4233–4246. (m) Nemykin, V. N.; Rohde, G. T.; Barrett, C. D.; Hadt, R. G.; Bizzarri, C.; Galloni, P.; Floris, B.; Nowik, I.; Herber, R. H.; Marrani, A. G.; Zanoni, R.; Loim, N. M. *J. Am. Chem. Soc.* **2009**, *131*, 14969–14978. (n) Galloni, P.; Floris, B.; de Cola, L.; Cecchetto, E.; Williams, R. M. *J. Phys. Chem. C* **2007**, *111*, 1517–1523. (o) Nemykin, V. N.; Rohde, G. T.; Barrett, C. D.; Hadt, R. G.; Sabin, J. R.; Reina, G.; Galloni, P.; Floris, B. *Inorg. Chem.* **2010**, *49*, 7497–7509.

(4) (a) Burrell, A. K.; Campbell, W.; Officer, D. L. *Tetr. Lett.* **1997**, *38*, 1249. (b) Burrell, A. K.; Campbell, W. M.; Officer, D. L.; Scott, S. M.; Gordon, K. C.; McDonald, M. R. *J. Chem. Soc., Dalton Trans.* **1999**, 3349. (c) Jiao, L.; Courtney, B. H.; Fronczek, F. R.; Smith, K. M. *Tetrahedron Lett.* **2006**, *47*, 501. (d) Wang, H. J. H.; Jaquinod, L.; Olmstead, M. M.; Vicente, M. G. H.; Kadish, K. M.; Ou, Z.; Smith, K. M. *Inorg. Chem.* **2007**, *46*, 2898.

(5) (a) Gryko, D. T.; Zhao, F.; Yasseri, A. A.; Roth, K. M.; Bocian, D. F.; Kuhr, W. G.; Lindsey, J. S. *J. Org. Chem.* **2000**, *65*, 7356. (b) Schmidt, E. S.; Calderwood, T. S.; Bruice, T. C. *Inorg. Chem.* **1986**, *25*, 3718. (c) Cheng, K.-L.; Li, H.-W.; Ng, D. K. P. *J. Organomet. Chem.* **2004**, *689*, 1593. (d) Giasson, R.; Lee, E. J.; Zbao, X.; Wrighton, M. S. *J. Phys. Chem.* **1993**, *97*, 2596. (e) Muraoka, T.; Kinbara, K.; Aida, T. *Nature* **2006**, *440*, 512. (f) Maiya, G. B.; Barbe, J. M.; Kadish, K. M. *Inorg. Chem.* **1989**, *28*, 2524–2527. (h) Solntsev, P. V.; Sabin, J. R.; Dammer, S. J.; Gerasimchuk, N. N.; Nemykin, V. N. *Chem. Commun.* **2010**, *46*, 6581–6583.

(6) (a) Gryko, D. T.; Piechowska, J.; Jaworski, J. S.; Galezowski, M.; Tasior, M.; Cembor, M.; Butenschoen, H. *New J. Chem.* **2007**, *31*, 1613–1619. (b) Venkatraman, S.; Kumar, R.; Sankar, J.; Chandrashekar, T. K.; Sendhil, K.; Vijayan, C.; Kelling, A.; Senge, M. O. *Chem.—Eur. J.* **2004**, *10*, 1423–1432.

(7) (a) Nemykin, V. N.; Kobayashi, N. *Chem. Commun.* **2001**, 165–166. (b) Lukyanets, E. A.; Nemykin, V. N. *J. Porphyrins Phthalocyanines* **2010**, *14*, 1–40.

(8) (a) Jin, Z.; Nolan, K.; McArthur, C. R.; Lever, A. B. P.; Leznoff, C. C. *J. Organomet. Chem.* **1994**, *468*, 205–12. (b) Poon, K.-W.; Yan, Y.; Li, X. Y.; Ng, D. K. P. *Organometallics* **1999**, *18*, 3528. (c) Salan, U.; Altindal, A.; Bulut, M.; Bekaroglu, O. *J. Porphyrins Phthalocyanines* **2006**, *10*, 1263–1270. (d) Nemykin, V. N.; Lukyanets, E. A. In *Handbook of Porphyrin Science*; Kadish, K. K., Smith, K. M., Guilard, R., Eds.; World Scientific: Singapore, 2010; Vol. 3, pp 1−323. (e) Nemykin, V. N.; Lukyanets, E. A. *ARKIVOC* **2010**, (i), 136–208.

(9) (a) Bucher, C.; Devillers, C. H.; Moutet, J.-C.; Pecaut, J.; Royal, G.; Saint-Aman, E.; Thomas, F. *Dalton Trans.* **2005**, 3620–3631. (b) Gale, P. A.; Hursthouse, M. B.; Light, M. E.; Sessler, J. L.; Warriner, C. N.; Zimmerman, R. S. *Tetrahedron Lett.* **2001**, *42*, 6759–6762.

(10) (a) Grimm, B.; Hausmann, A.; Kahnt, A.; Seitz, W.; Spanig, F.; Guldi, D. M. In *Handbook of Poprhyrin Science*; Kadish, K. K., Smith, K. M., Guilard, R., Eds.; World Scientific: Singapore, 2010; Vol. 1, pp 133−219.

(11) (a) Miller, J. S.; Epstein, A. J. *Angew. Chem., Int. Ed.* **1994**, *33*, 385. (b) Epstein, A. J.; Miller, J. S. *Synth. Met.* **1996**, *80*, 231. (c) Barlow, S. *Inorg. Chem.* **2001**, *40*, 7047. (d) Barlow, S.; O'Hare, D. *Chem. Rev.* **1997**, *97*, 637. (e) Kaim, W.; Lahiri, G. K. *Angew. Chem., Int. Ed.* **2007**, *46*, 1778–1796. (f) Kaim, W.; Sarkar, B. *Coord. Chem. Rev.* **2007**, *251*, 584–594. (g) Chisholm, M. H.; Patmore, N. J. *Acc. Chem. Res.* **2007**, *40*, 19–27.

(12) Nemykin, V. N.; Rohde, G. T.; Barrett, C. D.; Hadt, R. G.; Sabin, J. R.; Reina, G.; Galloni, P.; Floris, B. *Inorg. Chem.* **2010**, *49*, 7497–7509.

(13) Frisch, M. J.; Trucks, G. W.; Schlegel, H. B.; Scuseria, G. E.; Robb, M. A.; Cheeseman, J. R.; Montgomery, J. A., Jr.; Vreven, T.; Kudin, K. N.; Burant, J. C.; Millam, J. M.; Iyengar, S. S.; Tomasi, J.; Barone, V.; Mennucci, B.; Cossi, M.; Scalmani, G.; Rega, N.; Petersson, G. A.; Nakatsuji, H.; Hada, M.; Ehara, M.; Toyota, K.; Fukuda, R.; Hasegawa, J.; Ishida, M.; Nakajima, T.; Honda, Y.; Kitao, O.; Nakai, H.; Klene, M.; Li, X.; Knox, J. E.; Hratchian, H. P.; Cross, J. B.; Bakken, V.; Adamo, C.; Jaramillo, J.; Gomperts, R.; Stratmann, R. E.; Yazyev, O.; Austin, A. J.; Cammi, R.; Pomelli, C.; Ochterski, J.; Ayala, P. Y.; Morokuma, K.; Voth, G. A.; Salvador, P.; Dannenberg, J. J.; Zakrzewski, V. G.; Dapprich, S.; Daniels, A. D.; Strain, M. C.; Farkas, O.; Malick, D. K.; Rabuck, A. D.; Raghavachari, K.; Foresman, J. B.; Ortiz, J. V.; Cui, Q.; Baboul, A. G.; Clifford, S.; Cioslowski, J.; Stefanov, B. B.; Liu, G.; Liashenko, A.; Piskorz, P.; Komaromi, I.; Martin, R. L.; Fox, D. J.; Keith, T.; Al-Laham, M. A.; Peng, C. Y.; Nanayakkara, A.; Challacombe, M.; Gill, P. M. W.; Johnson, B. G.; Chen, W.; Wong, M. W.; Gonzalez, C. Pople, J. A. *Gaussian 03*, revision C.02; Gaussian, Inc.: Wallingford, CT, 2004.

(14) Becke, A. D. *Phys. Rev. A* **1988**, *38*, 3098.

(15) Lee, C.; Yang, W.; Parr, R. G. *Phys. Rev. B* **1988**, *37*, 785.

(16) Wachters, A. J. H. *J. Chem. Phys.* **1970**, *52*, 1033.

(17) McLean, A. D.; Chandler, G. S. *J. Chem. Phys.* **1980**, *72*, 5639.

(18) Nemykin, V. N.; Basu, P. *VMOdes: Virtual Molecular Orbital description program for Gaussian, GAMESS, and HyperChem, Revision A 7.2*; Univeristy of Minnesota: Duluth, MN, 2003.

(19) (a) Nemykin, V. N.; Hadt, R. G.; Belosludov, R. V.; Mizuseki, H.; Kawazoe, Y. *J. Phys. Chem. A* **2007**, *111*, 12901–12913. (b) Peralta, G. A.; Seth, M.; Ziegler, T. *Inorg. Chem.* **2007**, *46*, 9111–9125. (c) De Luca, G.; Romeo, A.; Scolaro, L. M.; Ricciardi, G.; Rosa, A. *Inorg. Chem.* **2009**, *48*, 8493–8507.

(20) (a) Semencic, M. C.; Heinze, K.; Foerster, C.; Rapic, V. *Eur. J. Inorg. Chem.* **2010**, 1089–1097. (b) Roy, L. E.; Jakubikova, E.; Guthrie, M. G.; Batista, E. R. *J. Phys. Chem. A* **2009**, *113*, 6745–6750. (c) Romero, T.; Caballero, A.; Espinosa, A.; Tarraga, A.; Molina, P. *Dalton Trans.* **2009**, 2121–2129. (d) Helten, H.; Fankel, S.; Feier-Iova, O.; Nieger, M.; Espinosa Ferao, A.; Streubel, R. *Eur. J. Inorg. Chem.* **2009**, 3226–3237. (e) Pinjari, R. V.; Gejji, S. P. *J. Phys. Chem. A* **2008**, *112*, 12679–12686. (f) Fuentealba, M.; Garland, M. T.; Carrillo, D.; Manzur, C.; Hamon, J.-R.; Saillard, J.-Y. *Dalton Trans.* **2008**, 77–86. (g) Nemykin, V. N.; Maximov, A. Y.; Koposov, A. Y. *Organometallics* **2007**, *26*, 3138. (h) Nemykin, V. N.; Makarova, E. A.; Grosland, J. O.; Hadt, R. G.; Koposov, A. Y. *Inorg. Chem.* **2007**, *46*, 9591. (i) Herber, R. H.; Nowik, I.; Grossland, J. O.; Hadt, R. G.; Nemykin, V. N. *J. Organomet. Chem.* **2008**, *693*, 1850. (j) Nemykin, V. N.; Hadt, R. G. *Inorg. Chem.* **2006**, *45*, 8297–8307.

(21) Lundberg, M.; Siegbahn, P. E. M. *J. Chem. Phys.* **2005**, *122*, 224103.

(22) (a) Hieringer, W.; Goeling, A. *Chem. Phys. Lett.* **2006**, *419*, 557. (b) Irgibaeva, I.; Aldongarov, A.; Barashkov, N.; Schmedake, T. *Int. J. Quantum Chem.* **2008**, *108*, 2641–2647. (c) Gritsenko, O.; Baerends, E. J. *J. Chem. Phys.* **2004**, *121*, 655–660. (d) Dreuw, A.; Head-Gordon, M. *J. Am. Chem. Soc.* **2004**, *126*, 4007–4016. (e) Ziegler, T.; Krykunov, M. *J. Chem. Phys.* **2010**, *133*, 074104/1–074104/11. (f) Zhekova, H. R.; Seth, M.; Ziegler, T. *J. Phys. Chem. A* **2010**, *114*, 6308–6321. (g) Fan, J.; Autschbach, J.; Ziegler, T. *Inorg. Chem.* **2010**, *49*, 1355–1362. (h) Ziegler, T.; Seth, M.; Krykunov, M.; Autschbach, J. *J. Chem. Phys.* **2008**, *129*, 184114/1–184114/9. (i) Ziegler, T.; Seth, M.; Krykunov, M.; Autschbach, J.; Wang, F. *J. Chem. Phys.* **2009**, *130*, 154102/1–154102/8.

JP1083828